A Mathematical Representation of the Wheatley Heart Valve

McKee, Sean; Cuminato, José Alberto; Stewart, Iain; Wheatley, David

Published in:
Journal of Biomechanical Engineering

DOI:
10.1115/1.4050753

Publication date:
2021

Document Version
Peer reviewed version

Journal of Biomechanical Engineering. Received July 09, 2020;
Accepted manuscript posted April 5, 2021. doi:10.1115/1.4050753

A Mathematical Representation of the Wheatley Heart Valve

S. McKee
Department of Mathematics and Statistics
University of Strathclyde
Glasgow,UK
Email: sean.mckee@strath.ac.uk

J. A. Cuminato*
Department of Applied Mathematics and Statistics
Universidade de São Paulo
São Carlos, SP, Brazil
Email: jacumina@icmc.usp.br

I. W. Stewart
Department of Mathematics and Statistics
University of Strathclyde
Glasgow, UK
Email: i.w.stewart@strath.ac.uk

D. J. Wheatley
School of Science and Engineering
University of Dundee
Dundee, UK
Email: david.j.wheatley@ntlworld.com

ABSTRACT

Starting from a hand-drawn contour plot, this note develops a set of intersecting and contiguous circles whose perimeter, upon extending appropriately to three dimensions, can be seen to be a natural mathematical representation of the Wheatley heart valve.

1 Introduction

The background and motivation for this study arise from the experience of one of the authors (DJW) as a clincal and academic cardiac surgeon with decades of experience of heart valve disease in different parts of the world and an international role through the European Association for Cardio-thoracic Surgery [1]. He also has a longstanding research experience in the field of heart valve replacement surgery [2, 3]. Recent and ongoing work has culminated in a potential solution to the clinical problems associated with current prosthetic heart valves, particularly in the developing world [4].

The majority of heart valve disease presents in the developing world where rheumatic fever is still prevalent. Currently the mechanical valves available for surgical treatment of advanced irreparable valve disease require life-long anticoagulant or antiplatlet therapy to mitigate thrombo-embolic complications [5]. Such therapy is often impractical or unavailable for those patients in the developing world who are vulnerable to heart valve disease. The alternative biological valves are less at risk of thrombo-embolic complications but have more limited durability, especially in young patients who are in the majority presenting with valve disease in developing countries [6, 7].

*Corresponding author

Journal of Biomechanical Engineering. Received July 09, 2020;
Accepted manuscript posted April 5, 2021. doi:10.1115/1.4050753

The quest has been to design a prosthetic valve that would be sufficiently resistant to degradation in the body to offer the prospect of survival in excess of two decades or more, while at the same time not running an associated appreciable risk of thrombo-embolic complications attributable to abnormal flow conditions associated predominantly with mechanical valves [8]. Currently available biostable polyurethanes show promise of durability in the human body [9]. The novel design suggested by one of the authors (the Wheatley valve) is the subject of this paper [10–12]. The design arises from experience with flexible-leaflet biological and synthetic valve prostheses. However, it differs from the usual design of flexible-leaflet valves [13] as it is intended to interact with known flow patterns within the ascending aorta [14]. This interaction should facilitate leaflet opening and closing, as well as avoiding areas of abnormally high or low shear stress at the valve/blood interfaces and areas of poor washout of blood around the valve. The design is also intended to significantly reduce the stresses within the leaflet material that are inherent in the current designs modelled on the natural aortic valve. This is a further feature that offers a prospect of enhanced durability in comparison with many bioprosthetic and experimental synthetic, flexible-leaflet valves.

Producing a mathematical representation of the design is a *useful* first step before applying computational fluid dynamics to understand both the blood flow in the valve and the ascending aorta, and the internal leaflet stresses during valve function. This paper is therefore intended to characterize the shape of the Wheatley valve using simple mathematical functions.Of course, the shape could have been generated via splines, but the principal advantage of a mathematical representation is that it permits shape changes to be easily trialed. For example, there is no need for a linear increase in the vertical direction: any power of z may be employed, generating an infinite family. Furthermore, circles may be replaced by ellipses, thus generating an even greater number of potential valves, so that an optimal shape may be efficiently ascertained. Some illustrations are supplied.

2 The artificial aortic valve

The artificial valve is displayed in Figure 1. Figure 1(a) displays the contour lines drawn by Wheatley himself, while Figure 1(b) depicts the actual valve: this is the shape we wish

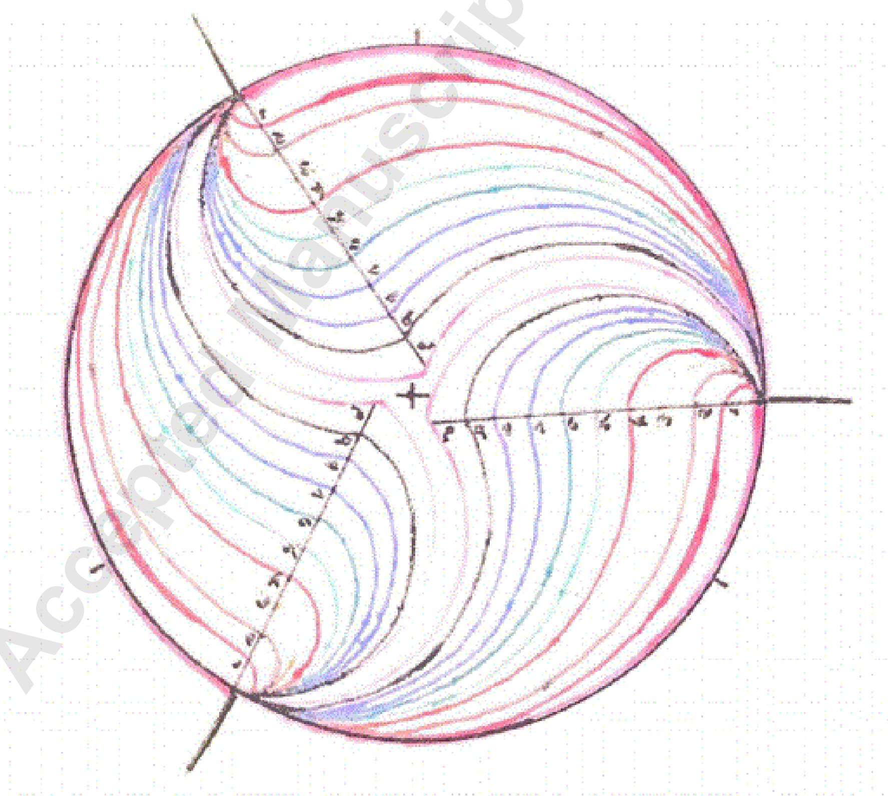

Fig. 1(a): Contour plots of the Wheatley valve

Journal of Biomechanical Engineering. Received July 09, 2020;
Accepted manuscript posted April 5, 2021. doi:10.1115/1.4050753

Fig. 1(b): The Wheatley Valve

to capture with simple mathematical functions. Indeed, close inspection of the valve and its associated contour lines suggests that, for each contour line, there exists six underlying symmetrically placed circles. These are displayed in Figure 2 with the appropriate arcs coloured red; the great circle is, for convenience and without any loss of generality, the unit circle. Note that the contours in Figure 1(a) are viewed from above the valve. The contour shown in Figure 2 is viewed from below and is therefore the mirror image.

3 Contiguous circles

Consider Figure 3. Note that C denotes the centre of the circle BPP' while S denotes the centre of the small circle BP''. Let $|OA| = a$ and $|OP''| = b$. From symmetry, we observe that $|OP| = |OP'| = b$. Then $|CB| = |CA| = (1+a)/2$ and $|P''S| = |SB| = (1-b)/2$. Furthermore, $|OC| = (1-a)/2$ and $|OS| = (1+b)/2$. In the X', Y'-coordinate system the equation of the circle BPP' is

$$\frac{x'^2}{\left[\frac{1}{2}(1+a)\right]^2} + \frac{y'^2}{\left[\frac{1}{2}(1+a)\right]^2} = 1. \tag{1}$$

Reverting to the X, Y-coordinate system this becomes

$$\frac{\left[x - \frac{1}{2}(1-a)\right]^2}{\left[\frac{1}{2}(1+a)\right]^2} + \frac{y^2}{\left[\frac{1}{2}(1+a)\right]^2} = 1. \tag{2}$$

Thus we see that the circle, provided by equation (2), passes through $B(1,0)$ and $A(-a,0)$; we wish it also to pass through $P(-\frac{1}{2}b, -\frac{\sqrt{3}}{2}b)$ and (and $P'(-\frac{1}{2}b, \frac{\sqrt{3}}{2}b)$, that is, we require

$$b^2 + \frac{1}{2}(1-a)b - a = 0 \tag{3}$$

or

$$a = \frac{b(2b+1)}{(2+b)}. \tag{4}$$

Journal of Biomechanical Engineering. Received July 09, 2020;
Accepted manuscript posted April 5, 2021. doi:10.1115/1.4050753

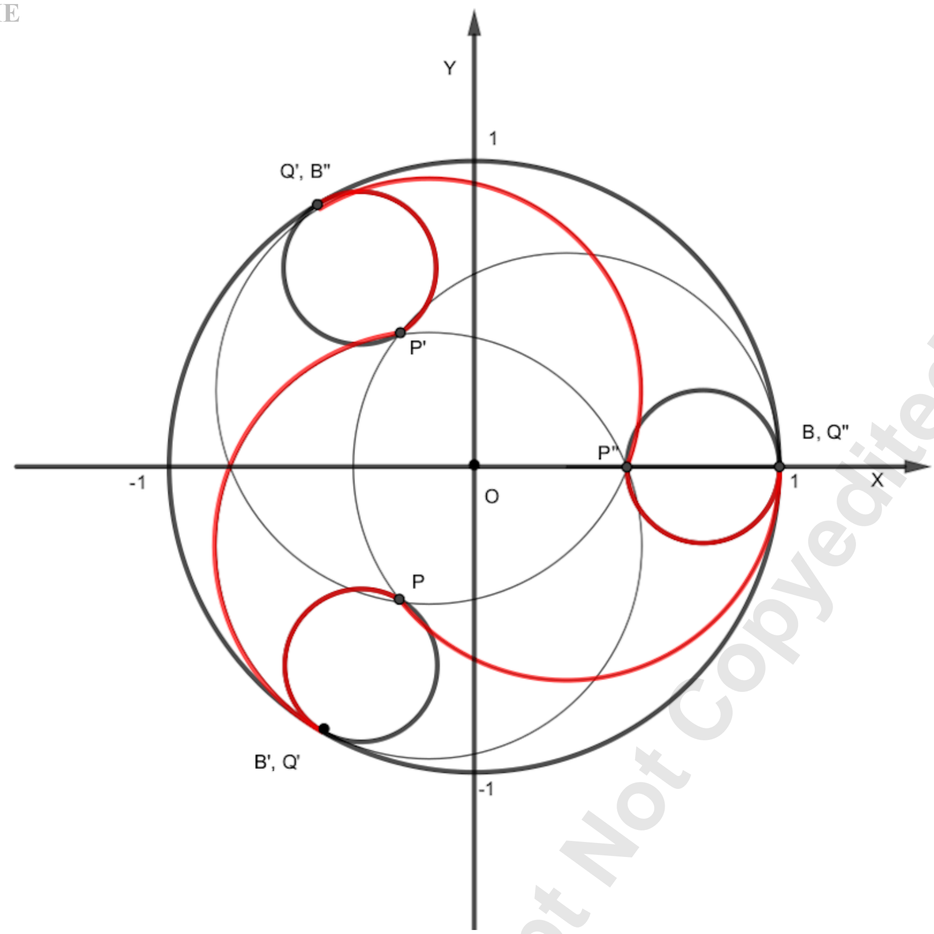

Fig. 2: Three larger and three smaller circles within the unit circle: the red line indicates the required arcs

Thus the circle, given by equation (2), now takes the form

$$\left(x-\frac{1-b^2}{2+b}\right)^2+y^2=\left(\frac{1+b+b^2}{2+b}\right)^2. \tag{5}$$

Further, since the radius of the circle BP'' is $\frac{1}{2}(1-b)$, its equation is given by

$$\left(x-\frac{1}{2}(1+b)\right)^2+y^2=\left(\frac{1}{2}(1-b\right)^2. \tag{6}$$

4 Two further sets of circles

We have established the equations of the two circles BPP' and BP'', given in Figure 3. However, from Figure 2 it is evident from symmetry that the two sets of circles $B'P'P''$ and PQ and $B''P''P$ and $P'Q'$ are exactly the same pairs of circles whose equations have already been developed: the only difference is that these pairs of circles have been rotated by $\frac{4}{3}\pi$ and $\frac{2}{3}\pi$, respectively.

4.1 Circles $B'P'P''$ and PQ

Consider Figure 4.

We note that, in the X',Y'-coordinate system, the equations for the circles $P'P''Q$ and PQ are, respectively,

Journal of Biomechanical Engineering. Received July 09, 2020;
Accepted manuscript posted April 5, 2021. doi:10.1115/1.4050753

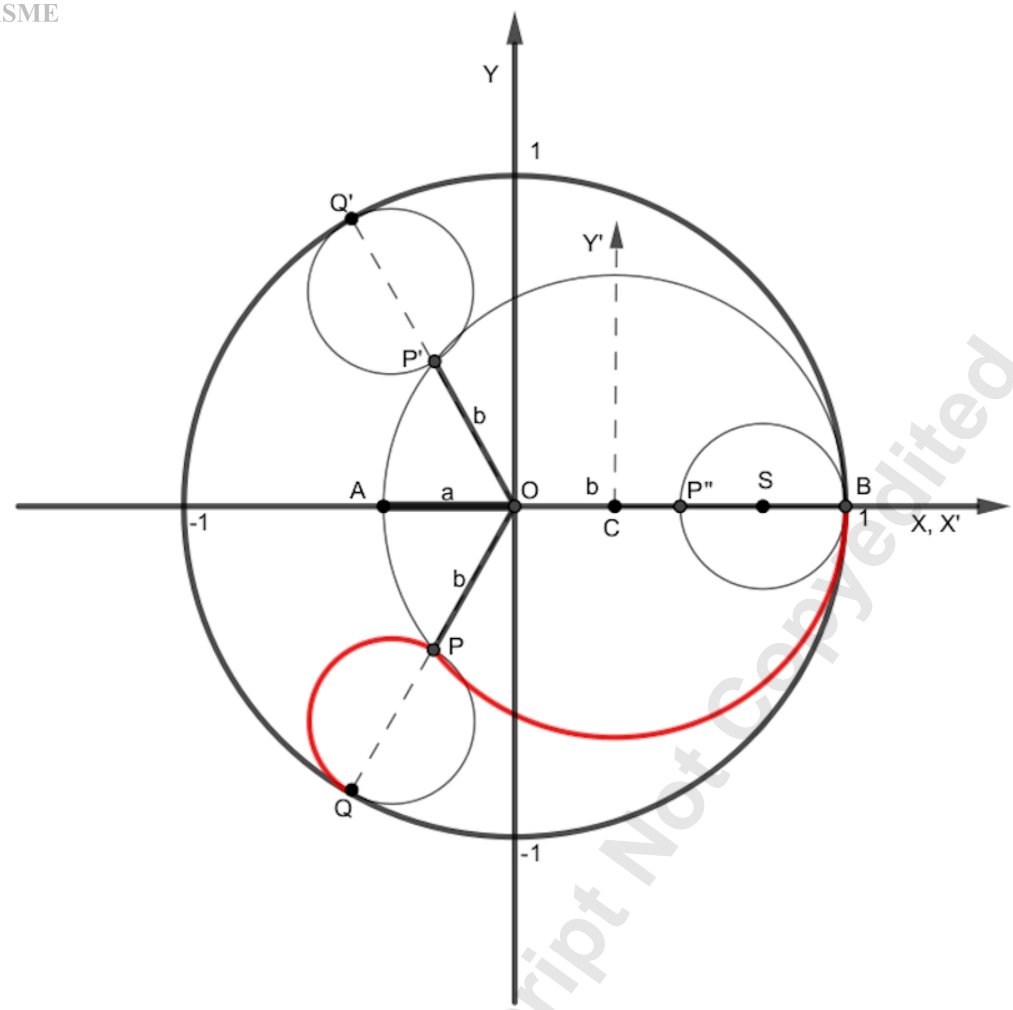

Fig. 3: A large circle and three smaller circles symmetrically placed around the origin

$$\left(x' - \frac{1-b^2}{2+b}\right)^2 + y'^2 = \left(\frac{1+b+b^2}{2+b}\right)^2 \tag{7}$$

and

$$\left(x' - \frac{1}{2}(1+b)\right)^2 + y'^2 = \left(\frac{1}{2}(1-b)\right)^2. \tag{8}$$

Now, clockwise axis rotation from (X', Y') to (X, Y) through $\frac{4}{3}\pi$ is given by

$$x' = \cos\frac{4}{3}\pi x + \sin\frac{4}{3}\pi y = -\frac{1}{2}x - \frac{\sqrt{3}}{2}y, \tag{9}$$

$$y' = -\sin\frac{4}{3}\pi x + \cos\frac{4}{3}\pi y = \frac{\sqrt{3}}{2}x - \frac{1}{2}y. \tag{10}$$

Journal of Biomechanical Engineering. Received July 09, 2020;
Accepted manuscript posted April 5, 2021. doi:10.1115/1.4050753

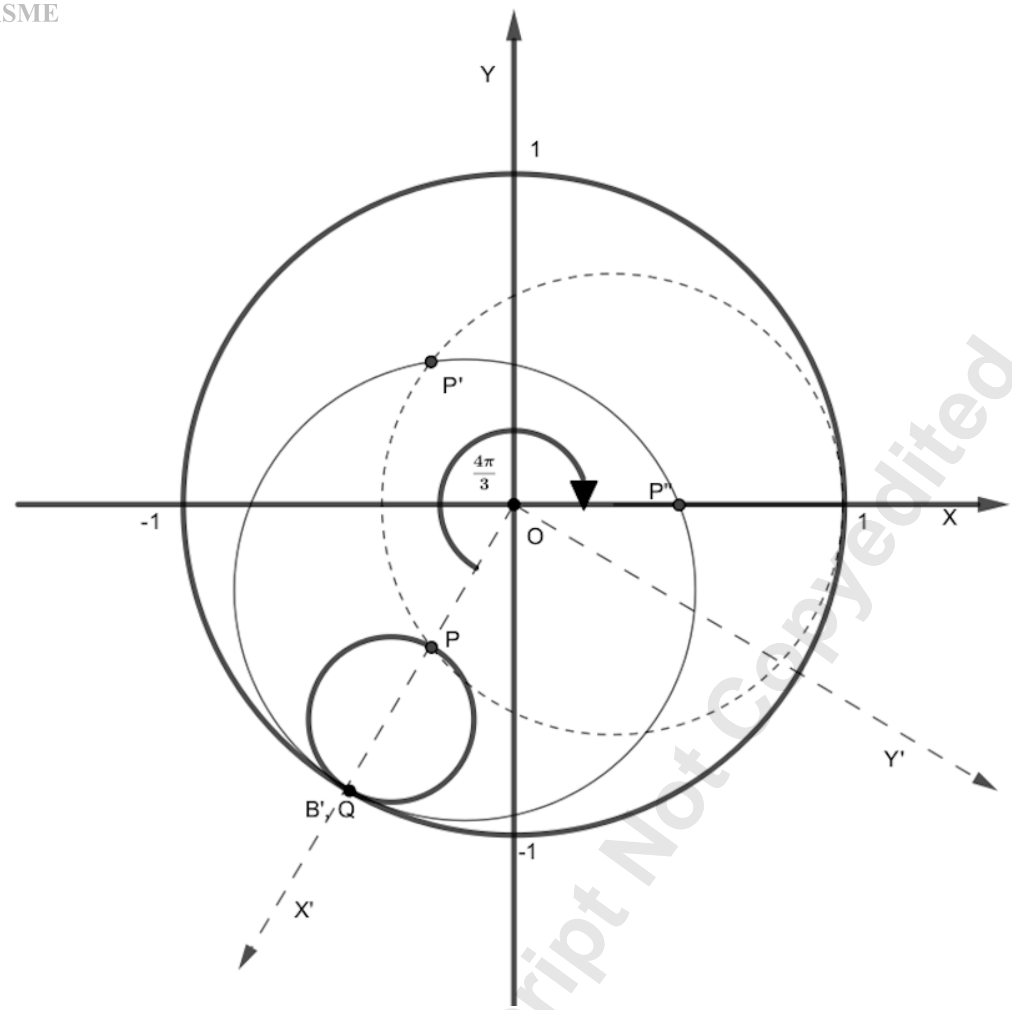

Fig. 4: Axes rotation through $\frac{4}{3}\pi$

Thus equations (7) and (8) in the X,Y-coordinates become

$$\left(-\frac{1}{2}x-\frac{\sqrt{3}}{2}y-\frac{1-b^2}{2+b}\right)^2+\left(\frac{\sqrt{3}}{2}x-\frac{1}{2}y\right)^2=\left(\frac{1+b+b^2}{2+b}\right)^2 \tag{11}$$

and

$$\left(-\frac{1}{2}x-\frac{\sqrt{3}}{2}y-\frac{1}{2}(1+b)\right)^2+\left(\frac{\sqrt{3}}{2}x-\frac{1}{2}y\right)^2=\left(\frac{1}{2}(1-b)\right)^2. \tag{12}$$

4.2 Circles $B''P''P$ and $P'Q'$

Similarly to the previous subsection, we note that the circles $Q'P''P'$ and $P'Q'$ can be expressed in the X',Y'-coordinate system displayed in Figure 5:

$$\left(x'-\frac{1-b^2}{2+b}\right)^2+y'^2=\left(\frac{1+b+b^2}{2+b}\right)^2 \tag{13}$$

and

Journal of Biomechanical Engineering. Received July 09, 2020;
Accepted manuscript posted April 5, 2021. doi:10.1115/1.4050753

$$\left(x' - \frac{1}{2}(1+b)\right)^2 + y'^2 = \left(\frac{1}{2}(1-b)\right)^2. \tag{14}$$

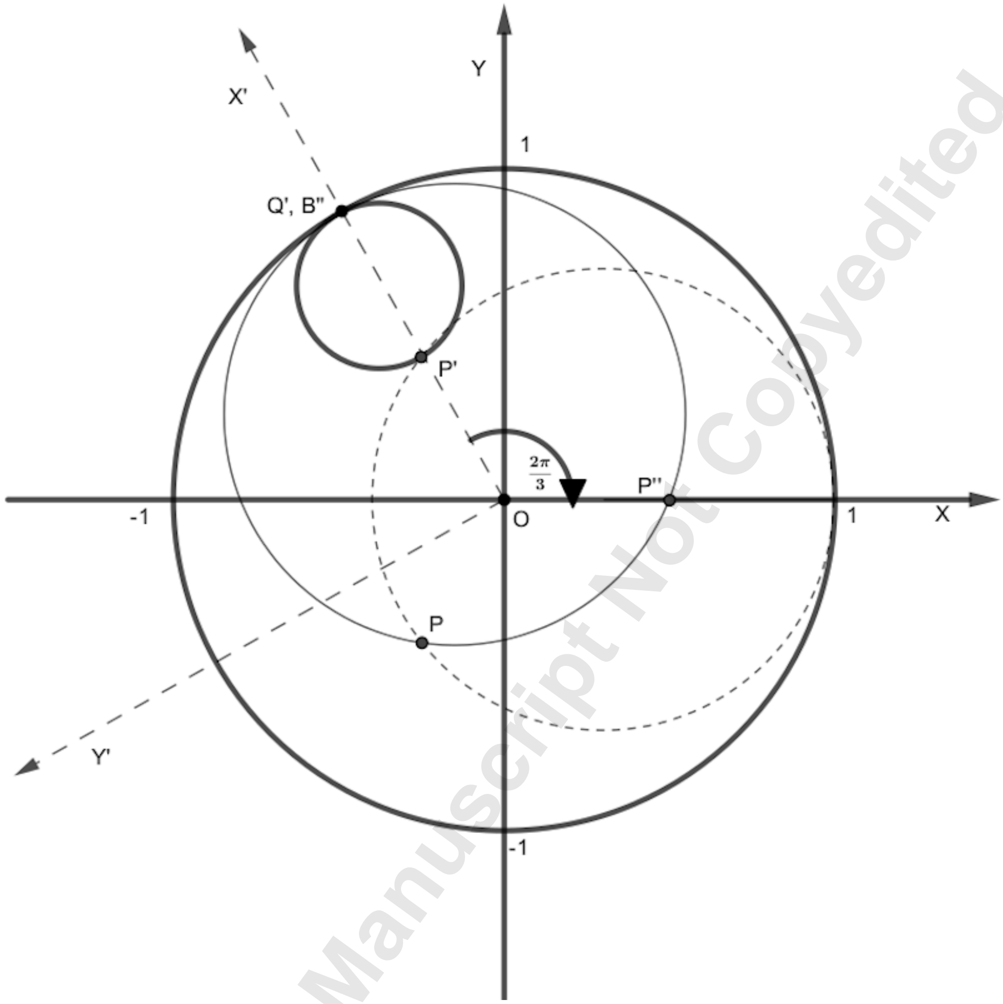

Fig. 5: Axes rotation through $\frac{2}{3}\pi$

As we can see from Figure 5 we require to rotate from (X', Y') to (X, Y) clockwise through $\frac{2}{3}\pi$. This is given by the transformation

$$x' = \cos\frac{2}{3}\pi x + \sin\frac{2}{3}\pi y = -\frac{1}{2}x + \frac{\sqrt{3}}{2}y, \tag{15}$$

$$y' = -\sin\frac{2}{3}\pi x + \cos\frac{2}{3}\pi y = -\frac{\sqrt{3}}{2}x - \frac{1}{2}y. \tag{16}$$

Thus equations (13) and (14) become

Journal of Biomechanical Engineering. Received July 09, 2020;
Accepted manuscript posted April 5, 2021. doi:10.1115/1.4050753

$$\left(-\frac{1}{2}x+\frac{\sqrt{3}}{2}y-\frac{1-b^2}{2+b}\right)^2+\left(-\frac{\sqrt{3}}{2}x-\frac{1}{2}y\right)^2=\left(\frac{1+b+b^2}{2+b}\right)^2 \tag{17}$$

and

$$\left(-\frac{1}{2}x+\frac{\sqrt{3}}{2}y-\frac{1}{2}(1+b)\right)^2+\left(\frac{\sqrt{3}}{2}x-\frac{1}{2}y\right)^2=\left(\frac{1}{2}(1-b)\right)^2. \tag{18}$$

In summary, the six circles, depicted in Figure 2, are given by the equations (5), (6), (11), (12), and (17) , (18).

5 Parametrization

For graphical purposes we require a parametrization of the six circles, that is, equations (5),(6),(11),(12), (17) and (18). Note that we wish to trace the arcs BP, PQ, $B'P'$, $P'Q'$, $B''P''$ and $P''Q''$ in the order indicated in Figure 2. Thus we shall examine the equations in the order (5), (12), (11), (18), (17) and (6).

For equation (5) we write the parametrization directly as

$$x-\frac{1-b^2}{2+b}=\frac{1+b+b^2}{2+b}\cos t,\; y=\frac{1+b+b^2}{2+b}\sin t, \tag{19}$$

For equation (12) we have

$$\left(\frac{\frac{1}{2}x+\frac{\sqrt{3}}{2}y+\frac{1}{2}(1+b)}{\frac{1}{2}(1-b)}\right)=\cos t,\;\left(\frac{\frac{\sqrt{3}}{2}x-\frac{1}{2}y}{\frac{1}{2}(1-b)}\right)=\sin t, \tag{20}$$

or

$$\frac{1}{2}x+\frac{\sqrt{3}}{2}y=-\frac{1}{2}(1+b)+\frac{1}{2}(1-b)\cos t, \tag{21}$$

$$\frac{\sqrt{3}}{2}x-\frac{1}{2}y=\frac{1}{2}(1-b)\sin t. \tag{22}$$

Solving the simultaneous equations yields

$$x=\frac{1}{4}\left\{-(1+b)+(1-b)\cos t+\sqrt{3}(1-b)\sin t\right\}, \tag{23}$$

$$y=\frac{1}{4}\left\{\sqrt{3}\left[-(1+b)+(1-b)\cos t\right]-(1-b)\sin t\right\}. \tag{24}$$

In a similar way we obtain the parametrization for equations (11),(18),(17) and (6) as, respectively,

Journal of Biomechanical Engineering. Received July 09, 2020;
Accepted manuscript posted April 5, 2021. doi:10.1115/1.4050753

$$x = \frac{1}{2}\left\{-\frac{1-b^2}{2+b} + \left(\frac{1+b+b^2}{2+b}\right)\cos t + \sqrt{3}\left(\frac{1+b+b^2}{2+b}\right)\sin t\right\}, \tag{25}$$

$$y = -\frac{1}{2}\left\{\sqrt{3}\left[\frac{1-b^2}{2+b} + \left(\frac{1+b+b^2}{2+b}\right)\cos t\right] + \left(\frac{1+b+b^2}{2+b}\right)\sin t\right\}, \tag{26}$$

$$x = \frac{1}{4}\left\{-(1+b) + (1-b)\cos t + \sqrt{3}(1-b)\sin t\right\}, \tag{27}$$

$$y = \frac{1}{4}\left\{\sqrt{3}\left[(1+b) + (1-b)\cos t\right] + (1-b)\sin t\right\}, \tag{28}$$

$$x = -\frac{1}{2}\left\{-\frac{1-b^2}{2+b} + \left(\frac{1+b+b^2}{2+b}\right)\cos t + \sqrt{3}\left(\frac{1+b+b^2}{2+b}\right)\sin t\right\}, \tag{29}$$

$$y = \frac{1}{2}\left\{\sqrt{3}\left[\frac{1-b^2}{2+b} + \left(\frac{1+b+b^2}{2+b}\right)\cos t\right] - \left(\frac{1+b+b^2}{2+b}\right)\sin t\right\}, \tag{30}$$

$$x = \frac{1}{2}\{1+b+(1-b)\cos t\}, \tag{31}$$

$$y = -\frac{1}{2}(1-b)\sin t. \tag{32}$$

6 Selecting the appropriate arcs

As already stressed we need to trace out, in the order, the arcs BP, PQ,$B'P'$,$P'Q'$, $B''P''$ and $P''Q''$. We therefore require the correct values of t for both the start and end values of each arc. Let t_B and t_P denote the start and end value for the arc BP, and t_P (generally different from the t_P for the arc BP) and t_Q denote the start and end value of the arc PQ with similar notation for the other remaining arcs. We obtain:

$$Arc\ BP : t_B = 2\pi,\ t_P = \pi + \cos^{-1}\left\{\frac{1+b-\frac{b^2}{2}}{1+b+b^2}\right\}, \tag{33}$$

$$Arc\ PQ : t_P = 2\pi,\ t_Q = \pi, \tag{34}$$

Journal of Biomechanical Engineering. Received July 09, 2020;
Accepted manuscript posted April 5, 2021. doi:10.1115/1.4050753

$$Arc\ B'P' : t_{B'} = 2\pi,\ t_{P'} = \pi + \cos^{-1}\left\{ -\frac{1+b-\frac{b^2}{2}}{1+b+b^2} \right\}, \tag{35}$$

$$Arc\ P'Q' : t_{P'} = 0,\ t_{Q'} = \pi, \tag{36}$$

$$Arc\ B''P'' : t_{B''} = 2\pi,\ t_{P''} = \pi + \cos^{-1}\left\{ \frac{1+b-\frac{b^2}{2}}{1+b+b^2} \right\}, \tag{37}$$

$$Arc\ P''Q'' : t_{P''} = -\pi,\ t_{Q''} = 0. \tag{38}$$

For the z-direction, we employ

$$z = \frac{b-\kappa}{1-\kappa} \tag{39}$$

and let b run from κ to 1. In this way z always belongs to $[0,1]$ while κ may be regarded as a measure of the degree of opening of the valve. In effect, we are stretching z so that it always lies in $[0,1]$ and removing part of the top of the valve. Thus the pictures in the next section provide only an indication as to how the valve might open; once the valve is subjected to spiral flow the leaflets are unlikely to open in unison as these pictures would appear to suggest.

7 Graphical results and discussion

The parameterized equations (19, 23-32) were used to produce graphs of the shape of the Wheatley valve (using MAPLE). Note that care is required to graph the correct arcs: those were determined by using the starting and end points given by (33-38). Pictures of the mathematical representation of the Wheatley valve are displayed in Figure 6. Note that Figure 6a shows the valve closed (during diastole) while Figure 6c-d show it opening (during systole) with Figure 6d displaying it fully open.

We can argue that this valve will be cheap to produce: if we consider the arcs as three sets of pairs, then we observe that the surface of each pair is topologically equivalent to a laminar sheet; this implies that the valve will not require a mould and therefore should not be expensive to produce.

However, it must be admitted that this mathematical representation is not entirely satisfactory in that there are lines on the leaflets where, although the surface is continuous, there is a sharp discontinuity in the derivative. In principle, this could be overcome by regularization, that is, by adding a smooth function across the discontinuity. Notwithstanding, we believe we have captured the essence of the Wheatley valve using very simple mathematical functions. It is rather pleasing, and unquestionably elegant, that the valve can be represented by an amalgamation of simple conic sections.

There is, however, scope for generalization: the z variable need not increase linearly - in Figure 7a z is replaced by z^2, while in Figure 7b z is replaced by z^4 displaying distinctly different shapes. In Figure 7c we show that the leaflets can be made to open separately by considering κ_1, κ_2 and κ_3 in place of the single κ; the spiral flow that emerges from the left ventricle will inevitably force the leaflets to open (and shut) at different rates. Finally, Figure 7d displays a valve with the circles replaced by ellipses, once again providing another distinct shape. Note that these four graphs, which are only illustrative of the possibilities, are shown (with the exception of 7c) in the shut position.

Journal of Biomechanical Engineering. Received July 09, 2020;
Accepted manuscript posted April 5, 2021. doi:10.1115/1.4050753

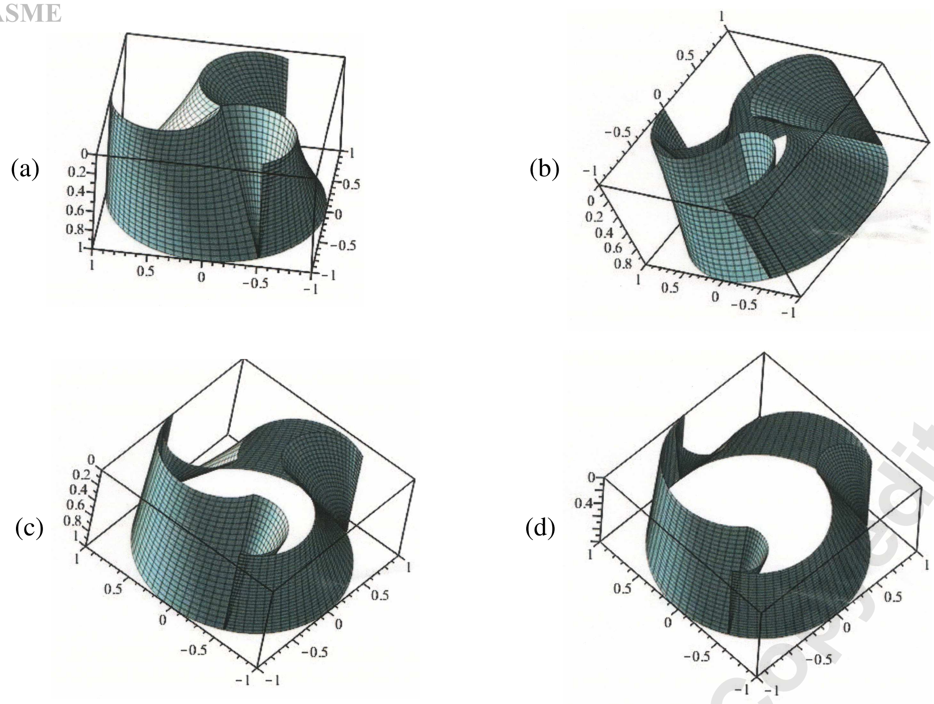

Fig. 6: Mathematical representation of the Wheatley valve during systole, displaying the valve opening

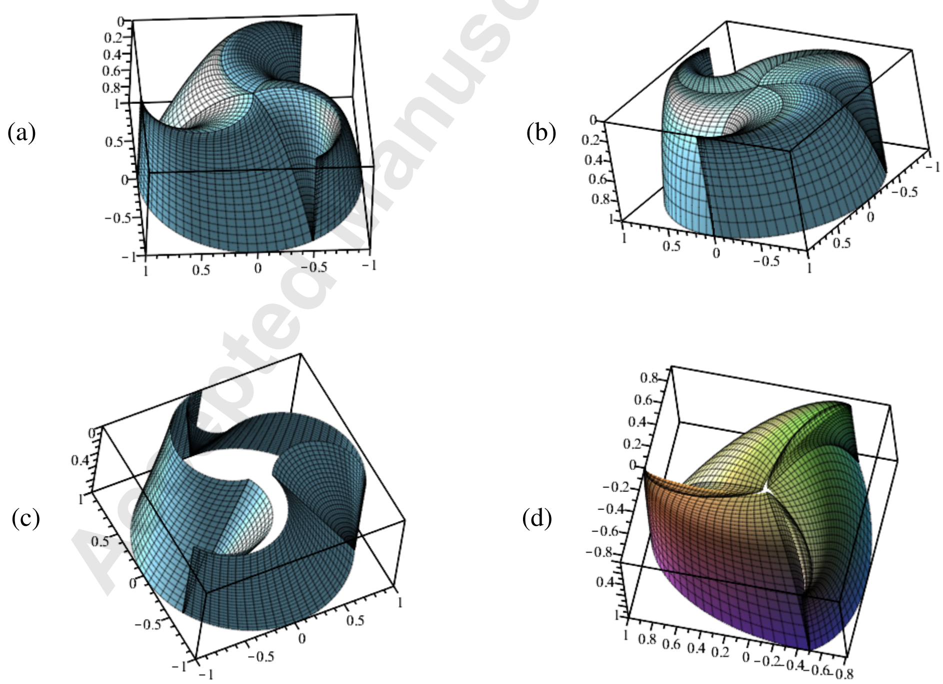

Fig. 7: (a) Wheatley valve with z replaced by z^2, (b) Wheatley valve with z replaced by z^4, (c) Wheatley valve with the leaflets opening separately (d) Wheatley valve with the circles replaced by ellipses.

Acknowledgements

The author J. A. Cuminato acknowledges the financial support of the funding agencies Fapesp (Grant #13/07375-0) and CNPq (Grant #02954/2015-5)

References

[1] Wheatley, D. J., 1999. "Presidential address. cardiothoracic surgery in Europe: politics, pressures and practice". *Eur J Cardiothorac Surg,* **16**(6), December, pp. 593–601.
[2] Wheatley, D. J., and McGregor, C. G. A., 1977. "Post implantation viability in canine allograft heart valves". *Cardiovac Res.,* **11**(1), January, pp. 78–85.
[3] Chaudhry, M. A., Raco, L., Muriithi, E. W., Bernacca, G. M., Tolland, M. M., and Wheatley, D. J., 2000. "Porcine versus pericardial bioprostheses: eleven-year follow-up of a prospective randomized trial". *J Heart Valve Dis,* **9**(3), May, pp. 429–437.
[4] Wheatley, D. J., Raco, L., Bernacca, G. M., Sim, I., Belcher, P. R., and Boyd, J. S., 2000. "Polyurethane: material for the next generation of heart valve prostheses?". *Eur J Cardiothorac Surg,* **17**(4), April, pp. 440–448.
[5] Oxenham, H., Bloomfield, P., Wheatley, D. J., Lee, R. J., Cunningham, J., Prescott, R. J., and Miller, H. C., 2003. "Twenty year comparison of bjork-shiley mechanical heart valve with porcine protheses". *Heart,* **89**(7), July, pp. 715–721.
[6] Zilla, P., Brink, J., Human, P., and Bezuidenhout, D., 2008. "Prosthetic heart valves: Catering for the few". *Biomaterials,* **29**(4), February, pp. 385–406.
[7] Howell, E. J., and Butcher, J. T., 2012. "Valvular heart diseases in the developing world: Developmental biology takes center stage". *J Heart Valve Dis,* **21**(2), March, pp. 234–240.
[8] Georgiadis, D., Kaps, M., Berg, J., MacKay, T. G., Dapper, F., Faichney, A., Wheatley, D. J., and Lees, K. R., 1996. "Transcranial doppler detection of microemboli in prosthetic heart valve patients: dependency upon valve type". *Eur J Cardiothorac Surg,* **10**(4), April, pp. 253–258.
[9] Wheatley, D. J., Bernacca, G. M., Tolland, M. M., O'Connor, B., Fisher, J., and Williams, D. F., 2001. "Hydrodynamic function of a biostable polyurethane flexible heart valve after 6 months in sheep". *Int J Artif Organs,* **24**(2), February, pp. 95–101.
[10] Wheatley, D. J., 2016. Heart valve. Published on grant. US Patent 9259313.
[11] Wheatley, D. J., 2017. Heart valve. Published on grant. UK Patent 2982340.
[12] Wheatley, D. J., 2017. Heart valve. Published on grant. European Patent 2979666.
[13] Ghanbari, H., Viatge, H., Kidane, A. G., Burriesci, G., Tavakoli, M., and Seifalian, A. M., 2009. "Polymeric heart valves: new materials, emerging hopes". *Trends Biotechnology,* **27**(6), June, pp. 359–367.
[14] Jarral, O. A., Tan, M. K. H., Salmasi, M. Y., Pirola, S., Pepper, J. R., O'Regan, D. P., Xu, X. Y., and Athanasiou, T., 2020. "Phase-contrast magnetic resonance imaging and computational fluid dynamics assessment of thoracic aorta blood flow: a literature review". *Eur J Cardiothorac Surg,* **57**(3), March, pp. 438–446.